

1 **Earth observation reveals reduced winter wheat growth and the
2 importance of plant available water during drought**

3 Hanna Sjulgård¹, Lukas Valentin Graf^{2,3}, Tino Colombi^{1,4}, Juliane Hirte³, Thomas Keller^{1,3,§}, Helge
4 Aasen^{3,§}

5 ¹ Department of Soil and Environment, Swedish University of Agricultural Sciences (SLU), Uppsala, Sweden

6 ² Crop Science, Institute for Agricultural Science, ETH Zurich, Zürich, Switzerland

7 ³ Department of Agroecology and Environment, Agroscope, Zürich, Switzerland

8 ⁴ School of Biosciences, University of Nottingham, Sutton Bonington, United Kingdom

9 § These authors contributed equally

10 *Correspondence to:* Hanna Sjulgård (hanna.sjulgard@slu.se)

11
12 **Abstract.** Drought poses increasing challenges to global food production. Knowledge about the influence of drought on crop
13 development and the role of soil properties for crop drought severity is important in drought risk analysis and for mitigating
14 drought impacts at the landscape level. Here, we tested if satellite images from Sentinel-2 could be used to assess the impacts
15 of drought on crop development and the influence of soil properties on crop drought responses at the landscape scale, and what
16 the responses were. As a case study, we assessed winter wheat growth on 13 fields belonging to commercial farmers in southern
17 Sweden in a dry year (2018) and a year with normal weather conditions (2021). To track crop growth, green leaf area index
18 (GLAI) was estimated from satellite imagery using a radiative transfer model. Proxies for winter wheat growth rate, peak
19 GLAI, and the timing of peak GLAI were derived from the GLAI development at the single field level. We then compared the
20 crop growth proxies between the two years, and related the year-to-year differences between fields to measured soil properties.
21 We found lower estimated growth rates, lower peak GLAI and earlier peak GLAI in the dry year compared to the year with
22 normal weather conditions. A higher peak GLAI in the dry year was related to a higher growth rate, and this was not shown in
23 the year with normal precipitation. Differences in crop development between years were large for some fields but small for
24 other fields, suggesting that soil properties play a role in crop response to drought. We found that fields with a higher plant
25 available water capacity had a higher growth rate in the dry year and smaller relative differences in growth rate between the
26 two years. This shows the importance of soils to mitigate drought conditions, which will likely become more relevant in an
27 increasingly drier climate. Our case study demonstrates that satellite derived crop growth proxies can identify crop responses
28 to drought events, and that satellite imagery can be used to discover impacts of soil properties on crop development at scales
29 relevant to commercial farming.

34 **1 Introduction**

35 Extreme weather events such as droughts have become more frequent and severe in recent years due to climate change, posing
36 challenges to global food and feed production (IPCC 2022). Drought is one of the main climatic constraints limiting crop
37 growth and crop productivity (Fahad et al. 2017; Matiu et al. 2017; Ru et al. 2023). Water is crucial for plant growth, and
38 plants can respond to water limitation through different mechanisms, such as reducing water losses through transpiration by
39 closing their stomata (Huang et al. 2020) or by reducing leaf area (Wasaya et al. 2023). In turn, the photosynthesis rate and
40 thus carbon acquisition decrease. Plants may also accelerate their development to complete the plant life cycle before the
41 occurrence of a severe water deficit (Abid et al. 2018; Seleiman et al. 2021). The impact of drought on crops is complex and
42 depends on several factors including the plant species and variety, the developmental stage of plants, the timing, duration and
43 severity of the drought (Gray and Brady 2016), as well as the properties of the soil (Bodner et al. 2015).

44 The capacity of soil to sustain plant growth and crop productivity is affected by biological, chemical and physical soil
45 properties, which collectively determine the soil conditions for plant growth (Stockdale et al. 2002). Soils that allow water to
46 infiltrate and can store sufficient amounts of water to sustain plant growth can mitigate drought conditions (Rockström 2003;
47 Bodner et al. 2015). Higher soil moisture may also benefit nutrient uptake during drought, while a water deficit could lead to
48 a lack of nutrients in crops as nutrients are mainly transported into plants through water uptake (He and Dijkstra 2014). Plant
49 roots must also be able to penetrate the soil to access water and nutrient resources, where a high penetration resistance, which
50 increases under dry conditions, could impede root growth and resource accessibility (Bengough et al. 2011; Colombi et al.
51 2018). Recent research also provides evidence that certain rhizosphere microbiomes might enhance plant growth during dry
52 conditions (Rolli et al. 2015; Rubin et al. 2017; de Vries et al. 2020). Therefore, soil properties are of high importance to
53 sustain crop growth during drought.

54 Plant growth dynamics can be quantified with ecophysiological properties such as the green leaf area index (GLAI), which is
55 the ratio of photosynthetically active leaf area to ground area (Watson 1947). Previous studies using field experiments
56 demonstrated that the influence of soil properties and soil-borne stress on plant growth can be detected using GLAI. For
57 example, positive relationships between GLAI and soil water content have been found (Chen et al. 2021), and GLAI at the
58 heading stage of spring barley has been shown to decrease with a high degree of soil compaction (Lipiec et al. 1991). The
59 growth rate estimated from GLAI has also been shown to be related to soil organic carbon and nitrogen contents (Hirooka et
60 al. 2017). In addition, the GLAI may vary by crop species, scales and environmental factors (Kang et al. 2002; Kang et al.
61 2016; Lawal et al. 2022), and there is still limited information about how soil properties affect crop GLAI development under
62 extreme weather conditions, at scales relevant to commercial agriculture (i.e., at the landscape scale). Pot and field plot
63 experiments are needed to understand single factors, but conducting research at larger scales is important to capture the
64 heterogeneity of environmental factors in the landscape.

65 Monitoring crop growth at the landscape scale can be done with satellite remote sensing, for example using the twin
66 constellation of Sentinel-2A and 2B. The Sentinel-2 multispectral sensors have been shown to be suitable for estimating GLAI

67 for different crop species (Clevers et al. 2017; Revill et al. 2019; Dong et al. 2020; Ali et al. 2021). One promising way to
68 interpret satellite data for ecophysiological traits is the use of radiative transfer models that describe the relationship between
69 leaf and canopy traits and spectral properties of plants using physical principles (Jacquemoud et al. 1996; Myneni et al. 1997;
70 Verhoef 1998). Thus, in contrast to the widely used vegetation indices, there is no need to establish empirical relationships
71 between vegetation indices and crop traits (Atzberger et al. 2011). Those empirical relationships are usually not transferable
72 in space and time, and hence not suitable for studies at the landscape scale. In addition, vegetation indices such as the widely
73 used Normalized Difference Vegetation Index (NDVI) saturate at low biomass levels (Myneni and Williams 1994; Prabhakara
74 et al. 2015), which is undesirable for a reliable and robust quantification of plant growth. The combination of satellite images
75 and radiative transfer models allows estimating GLAI on a large scale.

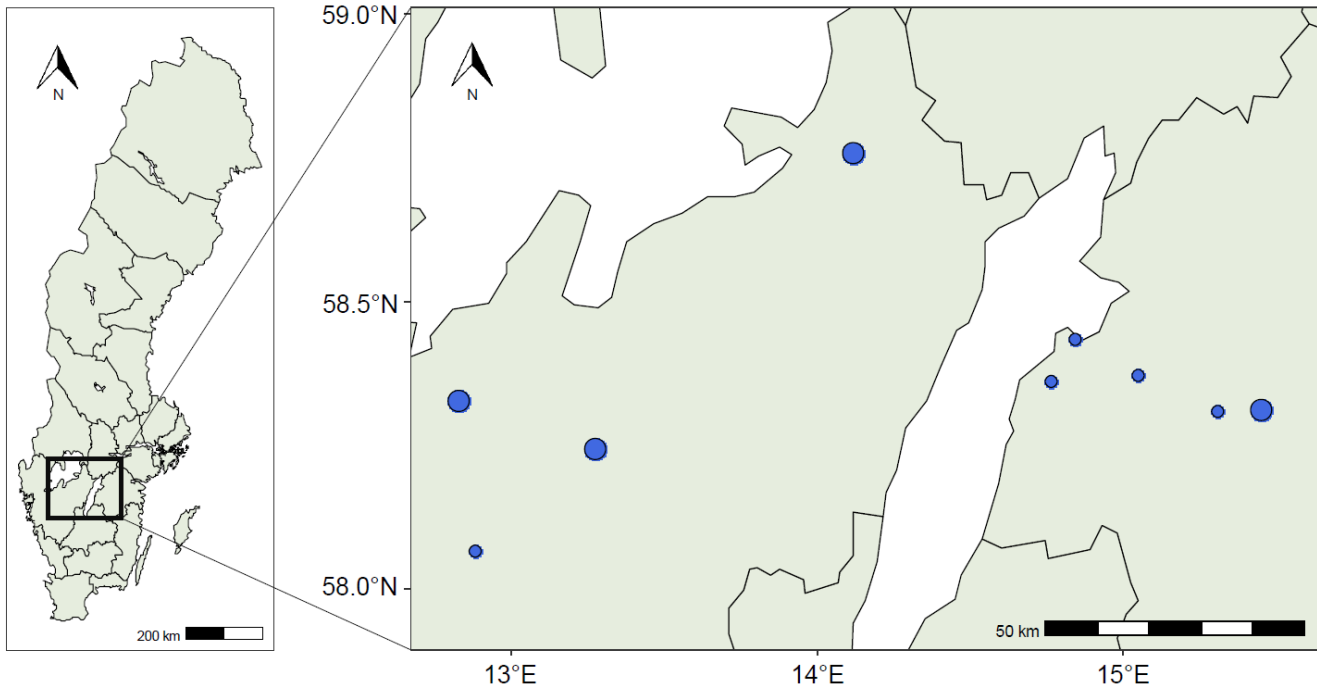
76 The use of satellite-derived GLAI for crop growth characterization and productivity has become common in recent years
77 (Punalekar et al. 2018; Peng et al. 2019; Dong et al. 2020; He et al. 2021; Graf et al. 2023), and many remote sensing studies
78 motivate their work by the potential of remote sensing to detect crop stress. Still, studies that a) demonstrate how extreme
79 weather, such as drought, affects GLAI development, and b) provide the link to environmental variables, such as soil properties,
80 to explain the observed differences remain scarce. Investigating if satellite images can be used to identify crop stress responses
81 at the landscape scale, and if the importance of soil properties can be identified under drought stress at agricultural fields, could
82 motivate the use of satellite images in crop monitoring at farm fields. In the present study, the aims were to:

- 83 i) analyse winter wheat development in farm fields within a region in southern Sweden by quantifying GLAI based on
84 Sentinel-2 data,
- 85 ii) investigate if impact of drought on winter wheat growth can be identified using satellite images at the farm fields by
86 comparing the GLAI development between a dry year (year 2018) and a year with normal weather conditions (year 2021), and
- 87 iii) examine if differences in soil properties relate to differences between GLAI development across fields and between
88 the two years.

89 **2 Materials and Methods**

90 **2.1 Study area and meteorological data**

91 The study area was located in the south of Sweden at a latitude of approximately 58.5°, spanning 160 km from west to east
92 (Fig. 1), and is characterized by a humid continental climate (Peel et al. 2007). Winter wheat is the major crop cultivated in
93 Sweden in general and in the study area (Sjulgård et al. 2022). We included 13 fields in this study, belonging to commercial
94 farmers. The fields were cultivated with winter wheat (*Triticum aestivum* L.) in both 2018 and 2021, and detailed soil data
95 were available for all fields. All fields were managed conventionally and they were not irrigated. The farmers manage their
96 fields according to best practices, but detailed information about crop and soil management practices was only available from
97 some of the farmers. We therefore minimised the variation in management practices between years by selecting fields that
98 were managed by the same farmer in 2018 and 2021, and with the same crop cultivated in both years.



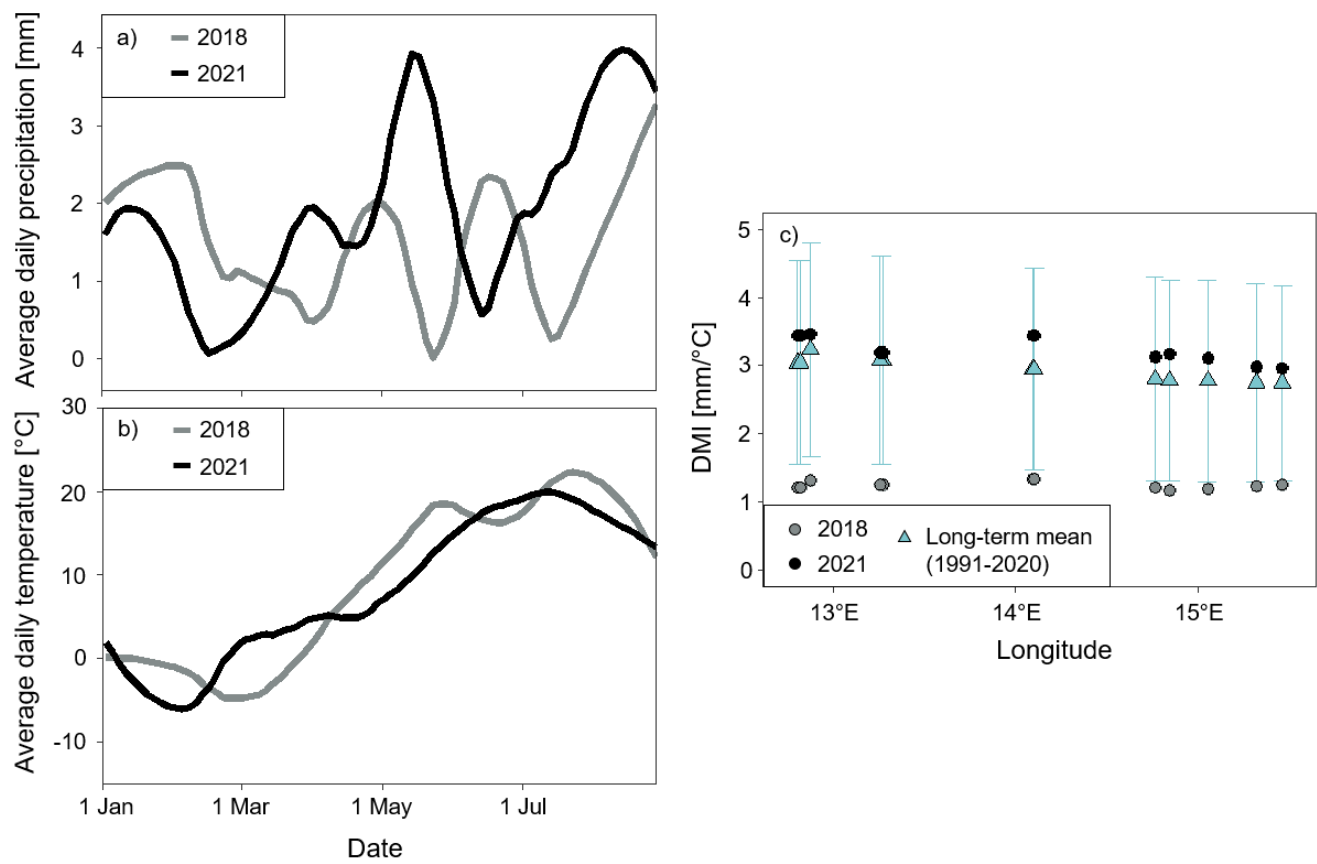
99
100 **Fig. 1. A map of Sweden with county borders showing the location of the study area (left), and a map displaying the locations of the**
101 **13 fields (right). A small blue circle indicates the location of one field, and a larger blue circle indicates two fields close to each other.**

102
103 The centroid coordinates of the fields were used to obtain daily temperature and precipitation data for each field.
104 Meteorological data were obtained from the “PTHBV database”, available from the Swedish Meteorological and Hydrological
105 Institute (SMHI). Data include gridded and interpolated daily mean temperature and precipitation at a resolution of 4 km by 4
106 km (SMHI 2023). The interpolation is based on 700 meteorological stations across Sweden and considers orographic effects
107 (Berg et al. 2015). Differences in weather conditions between fields and years were assessed by the De Martonne Aridity Index
108 (DMI; De Martonne 1926)), defined as:

109
110
$$DMI = \frac{P_m}{T_m + 10} \quad (1)$$

111
112 where P_m is the monthly total precipitation (mm) and T_m is the monthly average temperature (°C). A higher DMI indicates
113 wetter conditions, while a lower DMI indicates drier conditions. Weather conditions during the main winter wheat growing
114 period (May to July) in 2018 and 2021 were contrasting: 2018 was unusually dry, while 2021 was “normal” (Fig. 2). The lack
115 of precipitation has been referred to as the main reason for the large yield losses observed in 2018 (Bakke et al. 2020, Beillouin
116 et al. 2020). In 2018, May was already unusually warm and dry in Sweden (SMHI 2018). Between May and July, the DMI
117 was on average $1.2 \text{ mm } ^\circ\text{C}^{-1}$ ($SD = 0.06$) per month in 2018, which was drier than the long-term average of $2.9 \text{ mm } ^\circ\text{C}^{-1}$ (SD

118 = 0.19) for the same period. In 2021, the DMI was close to the long-term average with a monthly mean of $3.2 \text{ mm } ^\circ\text{C}^{-1}$ (SD =
119 0.16) in May to July. In both years, DMI was similar across fields.
120



121
122 **Fig. 2. Weather conditions in 2018 and 2021 at the locations of the 13 fields. Locally estimated scatterplot smoothing curves plotting**
123 **the average a) daily temperature and b) precipitation against calendar date for the 13 fields in 2018 and 2021. c) The average DMI**
124 **(De Martonne Aridity Index) during the months May to July in 2018 and 2021, and the long-term mean May to July between 1991**
125 **and 2020 with error bars indicating the standard deviation.**

126

127 **2.2 GLAI derived from satellite data**

128 The twin constellations of the Sentinel-2A and B satellites have a revisit time of two days in the study area. Downloading and
129 processing of Sentinel-2 data were performed using the open-source Python Earth Observation Data Analysis Library (EOdal,
130 Graf et al. 2022). The Sentinel-2 scenes were obtained for the years 2018 and 2021 from Microsoft Planetary Computer. 20 m
131 and 10 m bands were obtained, and the Sentinel-2 scenes and 20 m bands were resampled to 10 m using nearest-neighbour
132 interpolation to generate equal spatial resolution. The Sentinel-2 scenes were cropped to only retain pixels within the 13 fields
133 based on a shapefile containing the field boundaries. From the resampled scene classification layer, only pixels from the scene

classification layer class 4 (vegetation) and class 5 (bare soil) were kept to filter out pixels containing clouds, snow, shadow, and dark areas. Further filtering was performed to remove dates with a cloud cover of $\geq 10\%$ on a field-per-field basis. GLAI was derived from the radiative transfer model PROSAIL, following the approach described in Graf et al. (2023). A lookup table consisting of 50,000 spectra was generated by running PROSAIL in forward mode for each Sentinel-2 scene. We randomly generated combinations of leaf and canopy parameters according to a uniform or Gaussian distribution (Tab. S2; Graf et al. 2023; Wocher et al. 2020; Danner et al. 2021). View and illumination geometry were set to scene-specific values extracted from Sentinel-2 scene metadata. Building on the workflow of Graf et al. (2023), known empirical relationships between GLAI and chlorophyll a and b, and GLAI and the carotenoid content of leaves were used to increase the physiological plausibility of the input parameter combinations. For GLAI retrieval, we compared the Sentinel-2 pixel spectra with the PROSAIL simulated spectra using the mean absolute error as a cost function. We then used the median of the 5000 (10%) best matching simulated spectra in terms of the smallest mean absolute error to derive a GLAI value per Sentinel-2 pixel. For each Sentinel-2 scene, an average value of GLAI was calculated per field. A smoothed curve was fitted to the GLAI time series by the locally estimated scatterplot smoothing method with a span of 0.3 (Fig. 3). The smoothed curve was also used to identify and remove outliers that were missed by the scene classification layer and the cloud filtering (Fig. S1).

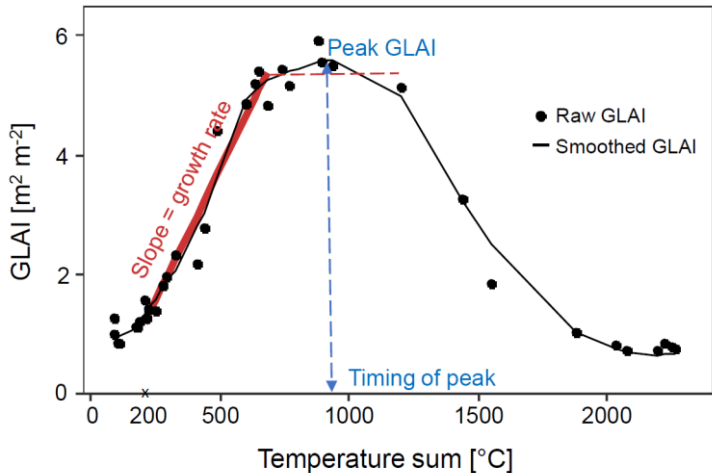
2.3 Crop growth curve parametrisation

The air temperature sum (T_{sum}) at each field was assessed by adding up the daily mean temperatures exceeding a threshold value of $0\text{ }^{\circ}\text{C}$, where growth for winter wheat starts (Porter and Gawith 1999), from the 1st of January following:

$$T_{\text{sum}} \text{UM} = \sum_{i=1}^j T_i \times \sigma_i$$

$$\sigma_i = \begin{cases} 0 & \text{if } T_i \leq 0\text{ }^{\circ}\text{C} \\ 1 & \text{if } T_i > 0\text{ }^{\circ}\text{C} \end{cases} \quad (2)$$

where T_i is the daily mean temperature and j is the number of days. From the GLAI development curve, characteristic properties were calculated to estimate crop growth rate, green biomass, and timing of heading stage for each field and year (Fig. 3). GLAI increases early in the season due to leaf production in the vegetative growth phase (Bhattacharya 2019). Growth rate during the vegetative growth phase was estimated from the slope of a linear plateau curve with an endpoint at the start of the upper plateau. The linear plateau model was fitted to the GLAI values with a start at a temperature sum of $200\text{ }^{\circ}\text{C}$ (corresponding to the end of April) when GLAI started to increase around the beginning of stem elongation (Chen et al. 2009). The GLAI development curve is typically bell-shaped, with the peak GLAI observed around the heading stage for winter wheat (Feng et al. 2019). The timing of the peak GLAI was assessed from the corresponding temperature sum (Fig. 3). The peak GLAI indicates the maximum green biomass (Lambert et al. 2018; Skakun et al. 2019), and was assessed from the smoothed GLAI curve.



164
165 **Fig. 3. Example from one of the fields showing the green leaf area index (GLAI) temporal development curve. We obtained proxies**
166 **for the growth rate from the slope between a temperature sum of 200 °C until the start of the plateau (dashed red line), the peak**
167 **GLAI from the maximum GLAI, and the timing of peak GLAI from the temperature sum at the peak GLAI. The raw GLAI values**
168 **are shown by black dots and the smoothed GLAI is shown by the black curve.**

169 **2.4 Soil sampling and analyses**

170 Soil sampling was conducted in June and in the beginning of July in 2021. Loose soil samples and undisturbed soil cores were
171 collected from the topsoil at five locations in each field. Sampling locations within each field were arranged in a quincunx,
172 with one point in the middle of the field and the others at least a few metres from the field borders. Loose soil samples were
173 taken with a shovel from 0-20 cm depth. The five samples taken in each field were pooled into a plastic bag and the resulting
174 composite sample was air-dried. Five undisturbed soil cores (5 cm in height, 7.2 cm inner diameter) were collected at a depth
175 of 10 cm in each field. The soil core samples were wrapped airtight and stored at 4 °C until further processing.

176 Soil organic matter content was determined by loss of ignition from the loose soil samples. Cation exchange capacity was
177 analysed using an inductively coupled plasma-optical emission spectrometer (ICP-OES) to obtain the base cations in the soil
178 samples. The base cations and acidity titration were used to calculate the cation exchange capacity at pH 7. Soil water content
179 at the permanent wilting point (-1500 kPa) was determined with pressure plate extractors. Soil water content at field capacity
180 was assessed by equilibrating the soil cores to -10 kPa (i.e., field capacity; Krueger and Ochsner (2024)) on ceramic plates
181 (ecoTec, Bonn). Plant available water capacity was obtained by calculating the difference in gravimetric soil water content
182 between field capacity and the permanent wilting point. Dry soil bulk density was determined on the undisturbed soil core
183 samples by drying the samples at 105 °C for 48 h. Soil texture including clay (< 0.002 mm) content was determined from the
184 loose soil samples by sedimentation ('pipette' method).

185 **2.5 Statistical analyses**

186 GLAI development responses to drought were analysed by comparing differences in crop growth proxies (i.e., growth rate,
187 peak GLAI, and the timing of peak) between the dry year (2018) and the year with normal weather conditions (2021). A two-
188 tailed t-test was applied to determine whether there was a significant difference in growth rate, peak GLAI, and the timing of
189 the peak GLAI between the two years. Spearman correlation was used to assess relationships between soil properties. Multiple
190 linear regression was used to assess relationships between the crop growth proxies while accounting for the average monthly
191 DMI (May – July) of the corresponding year. To relate soil properties to differences in growth rate, peak GLAI, and the timing
192 of the peak GLAI between years, the relative difference of crop growth proxies (ΔGP) between the years 2018 and 2021 was
193 calculated as:

194

195
$$\Delta GP = \frac{GP_{2021} - GP_{2018}}{GP_{2018}} \times 100\% \quad (3)$$

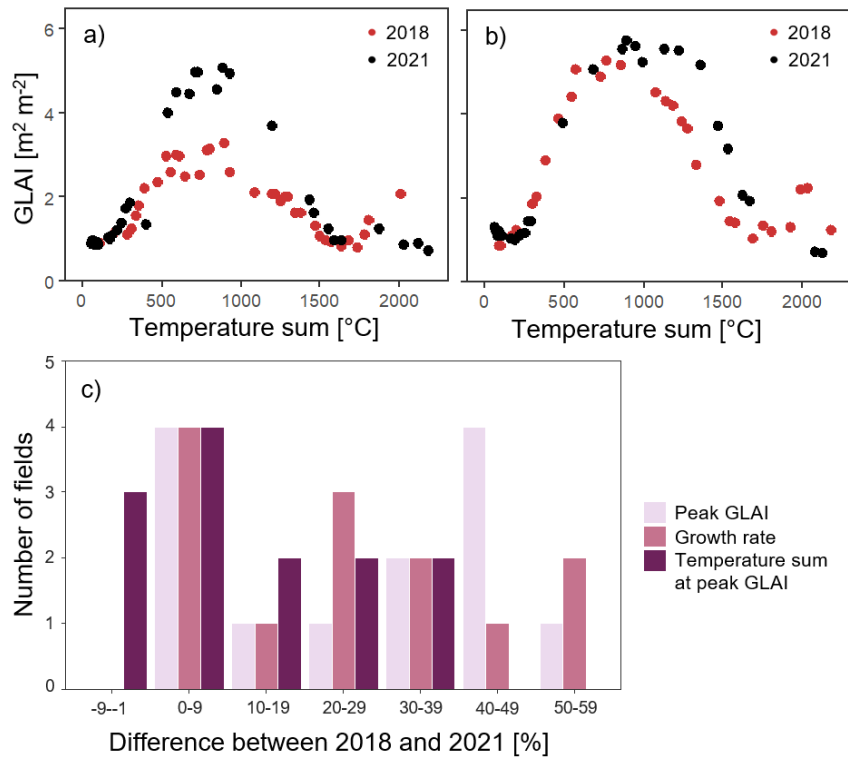
196

197 where GP is a crop growth proxy (i.e, growth rate, peak GLAI or the timing of the peak GLAI) for year 2018 and 2021.
198 A variance decomposition method proposed by Zuber and Strimmer (2011), called Correlation-Adjusted coRelation (CAR)
199 scores, was used to determine the relative importance of the soil properties for the growth rate, peak GLAI, and the timing of
200 the peak GLAI in each year (i.e., for 2021 and 2018), and for the relative difference of the crop growth proxies between the
201 years. CAR scores provide a criterion for variable ranking in linear regression based on the Mahalanobis-decorrelation of
202 covariates (Zuber and Strimmer 2011). The direction of the relationships and p-values were obtained from univariate linear
203 regressions between the crop growth proxies and the soil properties for each year, and for the relative difference of crop growth
204 proxies between 2021 and 2018, respectively. Statistical analyses were carried out in R version 4.2.1 (R Core Team 2022),
205 and CAR scores were calculated from the R package “relaimpo” (Groemping and Lehrkamp 2023) and the linear mixed models
206 using the “lme4” package (Bates et al. 2015).

207 **3 Results**

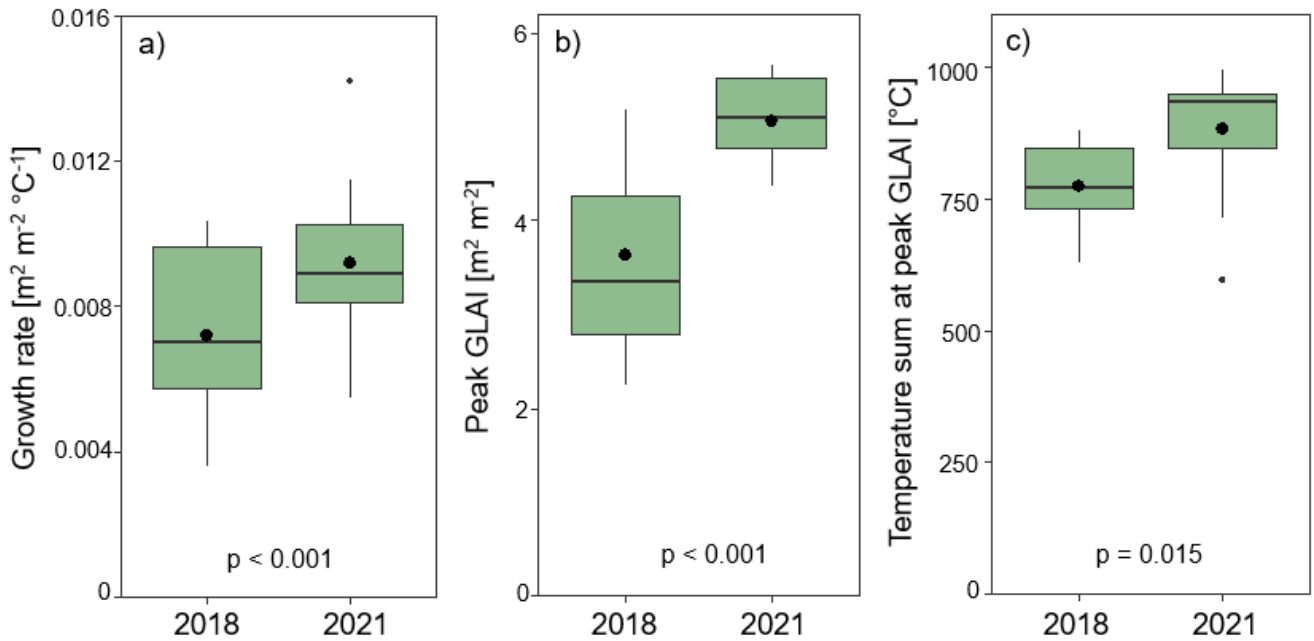
208 **3.1 Growth patterns across years**

209 Differences in crop development between years varied across fields, where certain fields showed a large difference in growth
210 rate, peak GLAI and the timing of the peak GLAI between years, while others had only small differences (Fig. 4, Fig. S2). For
211 growth rate and peak GLAI, four fields had an increase from 2018 to 2021 of less than 10%, while some fields had a difference
212 of 50-59%. The difference between years in the timing of the peak GLAI was lower in comparison, with four fields having an
213 increase <10% and three fields a decrease <10%, while the maximum difference was 30-39% (Fig. 4, Fig. S2).



214
215 **Fig. 4.** Examples of temporal evolution of GLAI during 2018 (dry year) and 2021 (year with normal weather conditions) for two
216 different fields with a) a large difference between the years and b) a small difference between the years. c) Number of fields by the
217 percentage difference in crop growth proxies (i.e., peak GLAI, growth rate, and temperature sum at peak GLAI) between the years
218 2018 (dry year) and 2021 (year with normal weather conditions).

219
220 Growth rate was lower in the dry year (2018) than in the year with normal weather conditions (2021; Fig. 5), indicating reduced
221 crop growth in response to drought. The growth rate during the reproductive period was on average 19% lower in the dry year
222 (2018) than in the year 2021 with close to normal weather conditions, and we found a significant effect of the year on growth
223 rate ($p < 0.001$; Fig. 5a). The peak GLAI was in general lower during the dry compared to the year with normal weather
224 conditions ($p < 0.001$; Fig. 5c), with an average difference of 28% between the two years. The timing of peak GLAI occurred
225 significantly earlier, i.e. at a lower temperature sum, during the dry year, with the peak GLAI around a temperature sum of
226 775 $^{\circ}\text{C}$ in the dry year and 881 $^{\circ}\text{C}$ in the year with normal weather conditions ($p = 0.015$; Fig. 5d).
227



228
229 **Fig. 5. Crop growth proxies obtained from the temporal evolution of green leaf area index (GLAI) in the dry year (2018) and the**
230 **year with normal weather conditions (2021); a) growth rate, b) peak GLAI, and c) temperature sum at peak GLAI. Data show yearly**
231 **average (black dots), median, upper and lower quartiles (box), and minimum and maximum values (whiskers). P-values from the t-**
232 **test are displayed for the differences between the years (number of fields, n=13).**

233 Relationships among the different crop growth proxies showed a positive relationship between growth rate and peak GLAI in
234 the dry year (year 2018), while the relationship was not significant during the year with normal weather conditions. The timing
235 of the peak GLAI had no significant relationship to growth rate or peak GLAI for either years (Tab. S3).

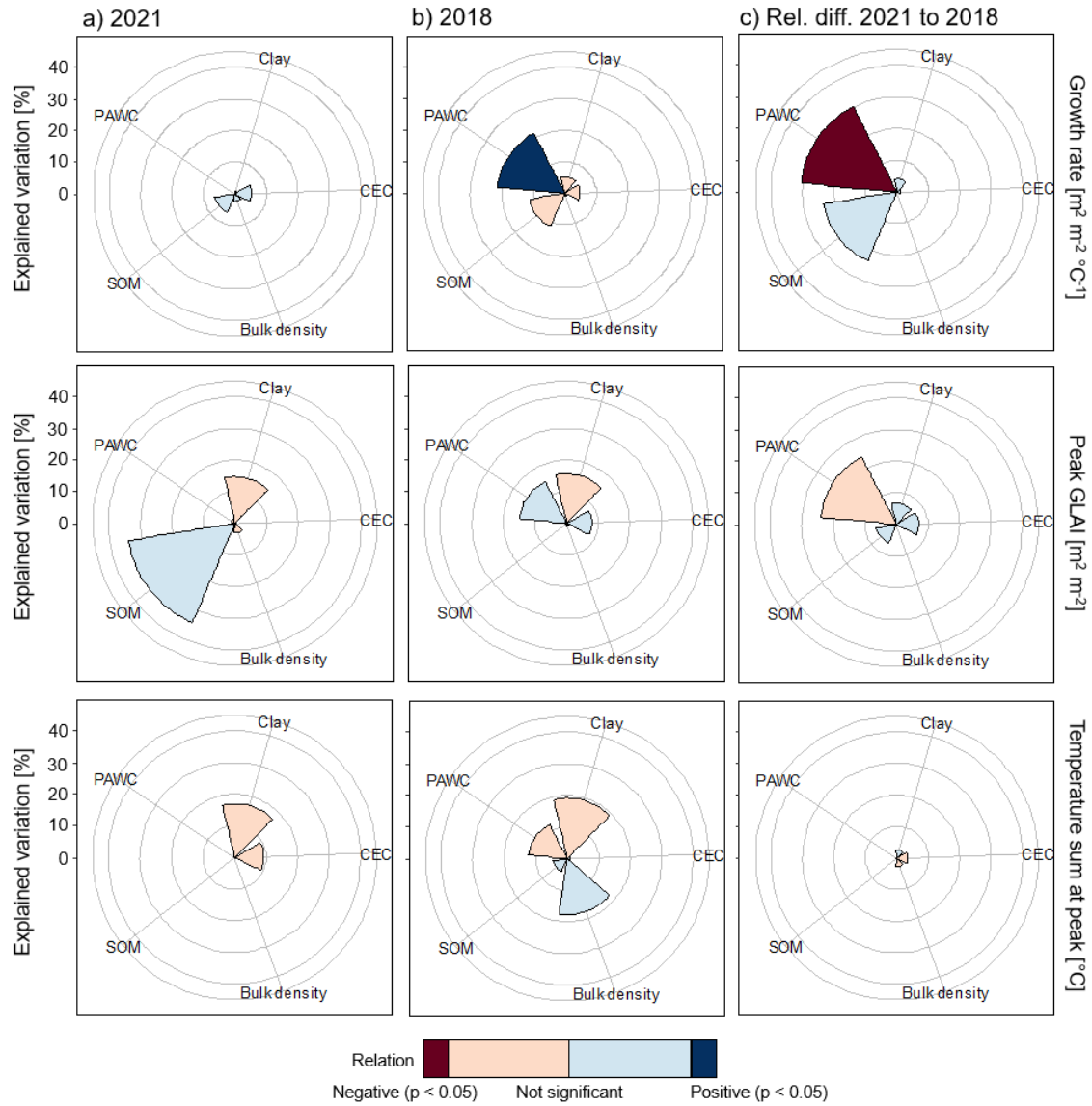
237 **3.2 Relationships between soil properties and crop development**

238 On average across the 13 fields, plant available water capacity was $0.23 \text{ m}^3 \text{ m}^{-3}$ bulk density was 1.5 g cm^{-3} , cation exchange
239 capacity was 16 cmol kg^{-1} , soil organic matter content was 3.6%, and clay content was 31% (Tab. S1). Some soil properties
240 were related to each other, with positive correlations between soil organic matter content and cation exchange capacity, and
241 between clay content and cation exchange capacity ($p < 0.05$; Fig. S4). Negative relationships were found between clay content
242 and bulk density, and between clay content and plant available water capacity ($p < 0.05$; Fig. S4).

243 Soil properties explained together 15%, 54% and 27% of the variations across fields in growth rate, peak GLAI, and timing of
244 peak GLAI, respectively, in the year with normal weather conditions (year 2021). However, none of the soil properties was
245 significantly related to growth rate, peak GLAI or timing of the peak GLAI in 2021 (Fig. 6a). In the dry year (year 2018), soil
246 properties explained together 44%, 40% and 55% of the variation in growth rate, peak GLAI and timing of peak GLAI,
247 respectively. Plant available water capacity was significantly related to crop growth rate in 2018, with a positive association

248 of increased crop growth with higher plant available water capacity ($p < 0.05$). In addition, plant available water capacity
 249 explained 21% of the variation in growth rate across fields in the dry year. There were no significant relationships between the
 250 other soil properties and growth rate, peak GLAI or timing of peak GLAI in 2018 (Fig. 6b). Plant available water capacity was
 251 the most important soil property in explaining the relative difference between the year with normal weather conditions (2021)
 252 and the dry year (2018). The relative difference in growth rate between the years was negatively related to plant available
 253 water capacity ($p < 0.05$), and plant-available water capacity explained 30% of the variation in the difference in growth rates
 254 between the years.

255



256

257 **Fig. 6. Explained variation in growth rate, peak GLAI and temperature sum at peak GLAI, calculated from correlation-adjusted**
258 **corelation (CAR) scores, by the soil properties clay content, soil organic matter content (SOM), bulk density, cation exchange**
259 **capacity (CEC) and plant available water capacity (PAWC) in a) a year with normal weather conditions (year 2021), b) a dry year**
260 **(year 2018), and c) the relative difference between the years 2021 and 2018. The p-values and the positive or negative relationships**
261 **between each soil property and crop growth proxy were obtained from univariate linear regressions. The rings are 10%, 20%, 30%**
262 **and 40% explained variation, starting from the smallest, and the last ring is the outside border of the plot area.**

263 **4 Discussion**

264 **4.1 The impact of drought on crop development**

265 In the present study, we used satellite images to assess winter wheat development in farm fields by quantifying GLAI based
266 on Sentinel-2 data. We investigated whether the impact of drought on GLAI development and relationships between soil
267 properties and GLAI development during drought could be identified by using satellite images. The early growing season in
268 2018 was exceptionally dry and warm (Fig. 2), resulting in reduced winter wheat development compared to 2021 (Fig. 5) that
269 had close to long-term average weather conditions. Previous research has shown negative effects of drought on crop yield at
270 the landscape and country scale (Zipper et al. 2016; Ray et al. 2018; Sjulgård et al. 2023), and lower growth rate and lower
271 peak GLAI during water-limited conditions have been found in field trials in which GLAI was measured at the canopy (Meinke
272 et al. 1997; Boedhram et al. 2001). The lower crop growth rate and the earlier GLAI peak during drought that we observed in
273 our study demonstrate that Sentinel-2 derived estimates of crop growth proxies can be used to detect drought responses in crop
274 development at the landscape scale.

275 The dry conditions early in the growing season in year 2018 resulted in lower peak GLAI compared to the year with normal
276 weather conditions (Fig. 5). Peak GLAI is a proxy of the maximum green biomass (Lambert et al. 2018; Skakun et al. 2019),
277 and reduced wheat biomass during drought has been shown in earlier studies (Villegas et al. 2001; Zhang et al. 2018).
278 According to Villegas et al. (2001), the decrease in biomass during drought was mainly due to a lower growth rate. Similarly,
279 we found a positive relationship between crop growth rate and peak GLAI in the dry year, but not in the year with normal
280 weather conditions (Tab. S3). The positive relationship in the dry year suggests that a faster growth is important to obtain
281 higher maximum biomass and in turn higher yield during dry conditions, and the non-significant relationship during the year
282 with normal weather conditions suggests that growth rate is not as critical for biomass accumulation during normal weather
283 conditions. Using farm fields, earlier research has shown that leaf area (He et al. 2020; Sun et al. 2024) and peak GLAI
284 (Lambert et al. 2018, Yamamoto et al. 2023) can be related to crop yield. For the fields with yield data available in this study
285 (six fields) together with additional 23 farm fields in the same region, there was a strong correlation between higher peak GLAI
286 and higher winter wheat yield in year 2021 shown in Sjulgård (2024). The peak GLAI was reached earlier, i.e., at a lower
287 temperature sum, during the dry year. Since the peak GLAI has been associated with heading growth stage (Feng et al. 2019),
288 this might indicate a shift in phenology during dry conditions. Some studies have shown that plants develop faster during
289 drought to reach flowering earlier and complete the life cycle before severe water shortage occurs (Abid et al. 2018; Seleiman
290 et al. 2021). However, we did not find a significant relationship between the timing of peak GLAI and growth rate or peak

291 GLAI in our data, which would imply that the timing of the heading growth stage did not influence the overall crop performance
292 (Tab. S3).

293 **4.2. The influence of soil properties on crop development**

294 We found that differences in crop development between the two years varied across fields. When comparing 2018 and 2021,
295 we identified a large difference of up to 50-59% in growth rate and peak GLAI for certain fields and up to 30-30% in the
296 timing of peak GLAI, while there was a smaller difference for other fields (Fig. 4, Fig. S2). As weather conditions across all
297 fields within a specific year were similar (Fig. 2c), the varying crop responses to drought stress among fields imply that
298 additional factors than the weather must have had an impact on crop development. Here, we show that soil properties influenced
299 the crop growth proxies. In 2018, a positive relationship between plant available water capacity and growth rate demonstrates
300 the importance of sufficient soil water retention to sustain crop growth during drought (Fig. 6). Fields with lower plant available
301 water capacity had a larger relative difference in growth rate between the dry and normal year. Earlier studies have shown that
302 soil water retention is crucial for crop performance during drought (Wang et al. 2009; Huang et al. 2020). Accordingly, the
303 performance of crops grown on soils with high plant available water capacity has been found less affected by changes in
304 rainfall compared to crops grown on soils with low plant available water capacity (Wang et al. 2017). The relevance of plant
305 available water capacity on crop growth during drought identified in our study demonstrates that the influence of soil properties
306 on crop development can be detected during drought stress at the landscape scale by using Sentinel-2 derived GLAI.

307 Other soil properties assessed in this study were not correlated with estimates of growth rate, peak GLAI or timing of peak
308 GLAI in 2018, and none of the soil properties was significantly related to the crop growth proxies in 2021 (Fig. 6). Clay content
309 only explained a small part of the variation in crop growth proxies, but influenced other soil properties such as cation exchange
310 capacity, bulk density, and plant available water capacity (Fig. S4). Cation exchange capacity only explained a low part of the
311 variation in crop growth proxies. All fields were above the recommended cation exchange capacity for crop production of 10
312 cmol kg^{-1} (Tab. S1) (Chowdhury et al. 2021), implying that cation exchange capacity was not a limiting factor for crop
313 development. Our findings that bulk density had no direct relationship with the crop growth proxies may seem to contradict
314 the study of Lipiec et al. (1991), who found decreasing GLAI at the heading stage of spring barley with increasing degree of
315 soil compaction. However, in our fields, bulk density was not critically high, with an average bulk density of 1.5 g cm^{-3} (Tab.
316 S1). We found no relationships between crop growth rate, peak GLAI or timing of peak GLAI and soil organic matter content.
317 Earlier studies have shown positive effects of soil organic matter content on soil fertility (Lal 2009; Fageria 2012; Oldfield et
318 al. 2019) and on crop productivity during drought (Kane et al. 2021; Mahmood et al. 2023), however, negative effects of soil
319 organic matter content on crop yields have also been found in Sweden (Kirchmann et al. 2020).

320 **4.3 Limitations and motivations**

321 In our study, soil sampling was conducted in 2021 only. With soil properties changing over time, this may introduce uncertainty
322 in the relationships between soil properties and crop development that we established for year 2018. However, a number of

323 studies has shown only small year-to-year changes in soil organic carbon content (Krauss et al. 2020), water content at field
324 capacity (Alam et al. 2014) and bulk density (Alam et al. 2014; Alnaimy et al. 2020) within given soil management systems.
325 The small differences between years suggests that the soil properties probably are rather similar between the years 2021 and
326 2018 within the same fields included in this study. In addition to soil properties and weather conditions, crop development is
327 influenced by soil and crop management practices such as fertilization (Agenbag and Maree 1991; Shankar et al. 2021), tillage
328 (Agenbag and Maree 1991; Abagandura et al. 2017), sowing date and crop variety selection (Ihsan et al. 2016; Minoli et al.
329 2022). Earlier studies have shown differences in leaf area index between farming systems, with higher leaf area index in
330 conventional in comparison to organic systems (Petcu et al. 2011; Pużyńska et al. 2021). In this study, all fields selected were
331 conventionally managed to reduce these differences. Additional information about the winter wheat varieties, sowing date and
332 fertilization levels were not available from all farmers. However, winter wheat is sown within a short time window around the
333 middle of September in the study region (Andersson 1983; SCB 1993). A change of a few days in sowing date of winter wheat
334 has been shown to have limited influence on crop yield (Ding et al. 2016), and would therefore not substantially influence our
335 findings. According to Stenberg et al. (2005), the average inorganic fertilizer used for winter wheat cultivation is 160 N kg ha⁻¹
336 (SD = 19) in Östergötland and 170 N kg ha⁻¹ (SD = 27) in Västra Götaland, respectively, based on extensive data collection
337 between 2000 and 2003. This shows that the fertilization levels between the two counties that covered our study region are
338 similar and that the variation between years is in general low.

339 The varying soil and crop management practices among fields, and the different availability of baseline data (e.g. soil
340 management and input history) is one of the challenges with on-farm research, but such studies are essential to evaluate the
341 use of satellite data in the context of commercial farms (Doole et al. 2023). Our results show that satellite derived GLAI can
342 be used to identify environmental stress response on plants, and this could help farmers to monitor crops and to identify when
343 stresses occur. The influence of soil properties on crop response during drought demonstrates the importance of accounting
344 for soil properties when evaluating the impact of drought on crops.

345 5 Conclusion

346 The impact of drought on winter wheat development was shown by comparing Sentinel-2 derived GLAI development during
347 a dry year (2018) and a year with normal weather conditions (2021) across 13 fields belonging to commercial farm fields in
348 southern Sweden. We observed lower crop growth rate, lower peak GLAI and earlier peak GLAI during the dry year compared
349 to the year with normal weather conditions. Our data revealed the importance of a faster crop growth to obtain more biomass
350 during dry conditions, while the growth rate was less crucial for crop performance during the year with normal weather
351 conditions. Differences in crop development between the years demonstrate that stress related crop response to changing
352 environmental conditions can be detected by monitoring crops using satellite images at the landscape level, and this could be
353 useful for farmers to monitor their crops and identify when the plants are stressed. In addition, we found that plant available
354 water capacity was important for crop growth rate during the dry year. This suggests that satellite imagery can be used to

355 discover soil impacts on crop development at scales relevant to commercial farming. The inclusion of soil properties in satellite
356 images analyses could further improve the accuracy of the prediction of drought stress on crops.

357 **Data availability**

358 The Sentinel-2 scenes were obtained from Microsoft Planetary Computer, and the downloading and processing were performed
359 using the open-source Python Earth Observation Data Analysis Library (EOdal, <https://github.com/EOA-team/eodal>). Data of
360 the growth proxies are available from the corresponding author upon request. The precipitation and temperature data are
361 available from the Swedish Meteorological and Hydrological Institute website <https://www.smhi.se/data/ladda-ner-data/griddade-nederbord-och-temperaturdata-pthby>.

363 **Author contributions**

364 Funding was acquired by TC, TK and HA. HS, TK and HA contributed to project conceptualization. HS performed the
365 investigations with advise from LVG, JH, TC, TK and HA. LVG implemented the programming code in Eodal. HS wrote the
366 paper, where the LVG, JH, TC, TK and HA contributed to the review and editing.

367 **Competing interests**

368 The contact author has declared that none of the authors has any competing interests.

369 **Acknowledgements**

370 This work was partly funded by the Swedish Farmers' Foundation for Agricultural Research (Stiftelsen Lantbruksforskning,
371 SLF, grant number: O-19-23-309) and by Formas (The Swedish Research Council for Sustainable Development; grant no:
372 2022-00218), which is greatly acknowledged. Hanna Sjulgård acknowledges financial support from the Lennart Hjelm's
373 foundation, Lukas Valentin Graf and Helge Aasen acknowledge funding by the Swiss National Science Foundation for the
374 project "PhenomEn" (grant number IZCOZ0_198091), and Tino Colombi acknowledges funding from the University of
375 Nottingham (Nottingham Research Fellowship). The authors want to thank all the farmers involved in this study for allowing
376 soil sampling on their fields. We also thank Laura Martínez, Leah Eitelberg and Loraine ten Damme for help with the soil
377 sampling, and Ana María Mingot Soriano, Anna Oskar and Jan Fiedler for laboratory measurements.

378
379

380 **References**

381 Abagandura GO, Nasr GE-DM, Moumen NM. 2017. Influence of Tillage Practices on Soil Physical Properties and Growth
382 and Yield of Maize in Jabal al Akhdar, Libya. Open Journal of Soil Science. 7(7):118–132.
383 <https://doi.org/10.4236/ojss.2017.77010>

384 Abid M, Ali S, Qi LK, Zahoor R, Tian Z, Jiang D, Snider JL, Dai T. 2018. Physiological and biochemical changes during
385 drought and recovery periods at tillering and jointing stages in wheat (*Triticum aestivum* L.). Sci Rep. 8:4615.
386 <https://doi.org/10.1038/s41598-018-21441-7>

387 Agenbag GA, Maree PCJ. 1991. Effect of tillage on some soil properties, plant development and yield of spring wheat
388 (*Triticum aestivum* L.) in stony soil. Soil and Tillage Research. 21(1):97–112. [https://doi.org/10.1016/0167-1987\(91\)90008-L](https://doi.org/10.1016/0167-1987(91)90008-L)

390 Alam MK, Islam MM, Saladin N, Hasanuzzaman M. 2014. Effect of Tillage Practices on Soil Properties and Crop Productivity
391 in Wheat-Mungbean-Rice Cropping System under Subtropical Climatic Conditions. The Scientific World Journal.
392 2014:e437283. <https://doi.org/10.1155/2014/437283>

393 Ali AM, Savin I, Poddubskiy A, Abouelghar M, Saleh N, Abutaleb K, El-Shirbeny M, Dokukin P. 2021. Integrated method
394 for rice cultivation monitoring using Sentinel-2 data and Leaf Area Index. The Egyptian Journal of Remote Sensing and Space
395 Science. 24(3, Part 1):431–441. <https://doi.org/10.1016/j.ejrs.2020.06.007>

396 Alnaimy M, Zelenakova M, Vranayova Z, Abu-Hashim M. 2020. Effects of Temporal Variation in Long-Term Cultivation on
397 Organic Carbon Sequestration in Calcareous Soils: Nile Delta, Egypt. Sustainability. 12(11):4514.
398 <https://doi.org/10.3390/su12114514>

399 Andersson B. 1983. Odlingstekniska försök med höstvete. Institutionen för Växtodling, Sveriges lantbruksuniversitet,
400 Uppsala.(121).

401 Atzberger C, Richter K, Vuolo F, Darvishzadeh R, Schlerf M. 2011. Why confining to vegetation indices? Exploiting the
402 potential of improved spectral observations using radiative transfer models. In: Remote Sensing for Agriculture, Ecosystems,
403 and Hydrology XIII. Vol. 8174. SPIE; p. 263–278. <https://doi.org/10.1117/12.898479>

404 Bakke SJ, Ionita M, Tallaksen LM. 2020. The 2018 northern European hydrological drought and its drivers in a historical
405 perspective. Hydrol Earth Syst Sci. 24(11):5621–5653. <https://doi.org/10.5194/hess-24-5621-2020>

406 Bates D, Mächler M, Bolker B, Walker S. 2015. Fitting Linear Mixed-Effects Models Using lme4. Journal of Statistical
407 Software. 67:1–48. <https://doi.org/10.18637/jss.v067.i01>

408 Beillouin D, Schauberger B, Bastos A, Ciais P, Makowski D. 2020. Impact of extreme weather conditions on European crop
409 production in 2018. Philos Trans R Soc Lond B Biol Sci. 375(1810):20190510. <https://doi.org/10.1098/rstb.2019.0510>

410 Bengough AG, McKenzie BM, Hallett PD, Valentine TA. 2011. Root elongation, water stress, and mechanical impedance: a
411 review of limiting stresses and beneficial root tip traits. Journal of Experimental Botany. 62(1):59–68.
412 <https://doi.org/10.1093/jxb/erq350>

413 Bhattacharya A. 2019. Chapter 3 - Water-Use Efficiency Under Changing Climatic Conditions. In: Bhattacharya A, editor.
414 Changing Climate and Resource Use Efficiency in Plants. Academic Press; p. 111–180. <https://doi.org/10.1016/B978-0-12-816209-5.00003-9>

415

416 Bodner G, Nakhforoosh A, Kaul H-P. 2015. Management of crop water under drought: a review. *Agron Sustain Dev.*
417 35(2):401–442. <https://doi.org/10.1007/s13593-015-0283-4>

418 Boedhram N, Arkebauer TJ, Batchelor WD. 2001. Season-Long Characterization of Vertical Distribution of Leaf Area in
419 Corn. *Agronomy Journal*. 93(6):1235–1242. <https://doi.org/10.2134/agronj2001.1235>

420

421 Chen S, Du T, Wang S, Parsons D, Wu D, Guo X, Li D. 2021. Quantifying the effects of spatial-temporal variability of soil
 422 properties on crop growth in management zones within an irrigated maize field in Northwest China. *Agricultural Water
 423 Management*. 244:106535. <https://doi.org/10.1016/j.agwat.2020.106535>

424 Chen Y, Carver BF, Wang S, Zhang F, Yan L. 2009. Genetic loci associated with stem elongation and winter dormancy release
 425 in wheat. *Theor Appl Genet*. 118(5):881–889. <https://doi.org/10.1007/s00122-008-0946-5>

426 Chowdhury S, Bolan N, Farrell M, Sarkar B, Sarker JR, Kirkham MB, Hossain MZ, Kim G-H. 2021. Chapter Two - Role of
 427 cultural and nutrient management practices in carbon sequestration in agricultural soil. In: Sparks DL, editor. *Advances in
 428 Agronomy*. Vol. 166. Academic Press; p. 131–196. <https://doi.org/10.1016/bs.agron.2020.10.001>

429 Clevers JGPW, Kooistra L, Van den Brande MMM. 2017. Using Sentinel-2 Data for Retrieving LAI and Leaf and Canopy
 430 Chlorophyll Content of a Potato Crop. *Remote Sensing*. 9(5):405. <https://doi.org/10.3390/rs9050405>

431 Colombi T, Torres LC, Walter A, Keller T. 2018. Feedbacks between soil penetration resistance, root architecture and water
 432 uptake limit water accessibility and crop growth – A vicious circle. *Science of The Total Environment*. 626:1026–1035.
 433 <https://doi.org/10.1016/j.scitotenv.2018.01.129>

434 Danner M, Berger K, Wocher M, Mauser W, Hank T. 2021. Efficient RTM-based training of machine learning regression
 435 algorithms to quantify biophysical & biochemical traits of agricultural crops. *ISPRS Journal of Photogrammetry and Remote
 436 Sensing*. 173:278–296. <https://doi.org/10.1016/j.isprsjprs.2021.01.017>

437 Ding DY, Feng H, Zhao Y, He JQ, Zou YF, Jin JM. 2016. Modifying Winter Wheat Sowing Date as an Adaptation to Climate
 438 Change on the Loess Plateau. *Agronomy Journal*. 108(1):53–63. <https://doi.org/10.2134/agronj15.0262>

439 Dong T, Liu Jiangui, Qian B, He L, Liu Jane, Wang R, Jing Q, Champagne C, McNairn H, Powers J, et al. 2020. Estimating
 440 crop biomass using leaf area index derived from Landsat 8 and Sentinel-2 data. *ISPRS Journal of Photogrammetry and Remote
 441 Sensing*. 168:236–250. <https://doi.org/10.1016/j.isprsjprs.2020.08.003>

442 Doole G, Tozer K, Sauermann C, Stevens D, Ward J. 2023. Challenges and opportunities for conducting on-farm research.
 443 *Journal of New Zealand Grasslands*.:85–93. <https://doi.org/10.33584/jnzb.2023.85.3659>

444 Fageria NK. 2012. Role of Soil Organic Matter in Maintaining Sustainability of Cropping Systems. *Communications in Soil
 445 Science and Plant Analysis*. 43(16):2063–2113. <https://doi.org/10.1080/00103624.2012.697234>

446 Fahad S, Bajwa AA, Nazir U, Anjum SA, Farooq A, Zohaib A, Sadia S, Nasim W, Adkins S, Saud S, et al. 2017. Crop
 447 Production under Drought and Heat Stress: Plant Responses and Management Options. *Frontiers in Plant Science*. 8.

448 Feng W, Wu Y, He L, Ren X, Wang Yangyang, Hou G, Wang Yonghua, Liu W, Guo T. 2019. An optimized non-linear
 449 vegetation index for estimating leaf area index in winter wheat. *Precision Agric*. 20(6):1157–1176.
 450 <https://doi.org/10.1007/s11119-019-09648-8>

451 Graf LV, Merz QN, Walter A, Aasen H. 2023. Insights from field phenotyping improve satellite remote sensing based in-
 452 season estimation of winter wheat growth and phenology. *Remote Sensing of Environment*. 299:113860.
 453 <https://doi.org/10.1016/j.rse.2023.113860>

454 Graf LV, Perich G, Aasen H. 2022. EOA-team/eodal_notebooks: EOdal Notebooks (Graf et al., 2022) [Internet]. [accessed
455 2023 Jul 20]. <https://doi.org/10.5281/ZENODO.7278252>

456 Gray SB, Brady SM. 2016. Plant developmental responses to climate change. *Developmental Biology*. 419(1):64–77.
457 <https://doi.org/10.1016/j.ydbio.2016.07.023>

458 Groemping U, Lehrkamp M. 2023. relaimpo: Relative Importance of Regressors in Linear Models [Internet]. [accessed 2023
459 Dec 22]. <https://cran.r-project.org/web/packages/relaimpo/index.html>

460 He L, Wang R, Mostovoy G, Liu Jane, Chen JM, Shang J, Liu Jiangui, McNairn H, Powers J. 2021. Crop Biomass Mapping
461 Based on Ecosystem Modeling at Regional Scale Using High Resolution Sentinel-2 Data. *Remote Sensing*. 13(4):806.
462 <https://doi.org/10.3390/rs13040806>

463 He M, Dijkstra FA. 2014. Drought effect on plant nitrogen and phosphorus: a meta-analysis. *New Phytologist*. 204(4):924–
464 931. <https://doi.org/10.1111/nph.12952>

465 He J, Shi Y, Zhao J, Yu Z, He J, Shi Y, Zhao J, Yu Z. 2020. Strip rotary tillage with subsoiling increases winter wheat yield
466 by alleviating leaf senescence and increasing grain filling. *Crop Journal*. 8(2):327–340.

467 Hirooka Y, Homma K, Maki M, Sekiguchi K, Shiraiwa T, Yoshida K. 2017. Evaluation of the dynamics of the leaf area index
468 (LAI) of rice in farmer's fields in Vientiane Province, Lao PDR. *J Agric Meteorol*. 73(1):16–21.
469 <https://doi.org/10.2480/agrmet.D-14-00021>

470 Huang Z, Liu Y, Tian F-P, Wu G-L. 2020. Soil water availability threshold indicator was determined by using plant
471 physiological responses under drought conditions. *Ecological Indicators*. 118:106740.
472 <https://doi.org/10.1016/j.ecolind.2020.106740>

473 Ihsan MZ, El-Nakhlawy FS, Ismail SM, Fahad S, daur I. 2016. Wheat Phenological Development and Growth Studies As
474 Affected by Drought and Late Season High Temperature Stress under Arid Environment. *Frontiers in Plant Science*. 7.

475 IPCC. 2022. Climate Change 2022: Impacts, Adaptation and Vulnerability Working Group II Contribution to the Sixth
476 Assessment Report of the Intergovernmental Panel on Climate Change. <https://doi.org/10.1017/9781009325844>

477 Jacquemoud S, Ustin SL, Verdebout J, Schmuck G, Andreoli G, Hosgood B. 1996. Estimating leaf biochemistry using the
478 PROSPECT leaf optical properties model. *Remote Sensing of Environment*. 56(3):194–202. [https://doi.org/10.1016/0034-4257\(95\)00238-3](https://doi.org/10.1016/0034-4257(95)00238-3)

479 Kane DA, Bradford MA, Fuller E, Oldfield EE, Wood SA. 2021. Soil organic matter protects US maize yields and lowers crop
480 insurance payouts under drought. *Environ Res Lett*. 16(4):044018. <https://doi.org/10.1088/1748-9326/abe492>

481 Kang S, Zhang F, Hu X, Zhang J. 2002. Benefits of CO₂ enrichment on crop plants are modified by soil water status. *Plant
482 and Soil*. 238(1):69–77. <https://doi.org/10.1023/A:1014244413067>

483 Kang Y, Özdoğan M, Zipper SC, Román MO, Walker J, Hong SY, Marshall M, Magliulo V, Moreno J, Alonso L, et al. 2016.
484 How Universal Is the Relationship between Remotely Sensed Vegetation Indices and Crop Leaf Area Index? A Global
485 Assessment. *Remote Sensing*. 8(7):597. <https://doi.org/10.3390/rs8070597>

487 Kirchmann H, Börjesson G, Bolinder MA, Kätterer T, Djodjic F. 2020. Soil properties currently limiting crop yields in Swedish
488 agriculture – An analysis of 90 yield survey districts and 10 long-term field experiments. *European Journal of Agronomy*.
489 120:126132. <https://doi.org/10.1016/j.eja.2020.126132>

490 Krauss M, Berner A, Perrochet F, Frei R, Niggli U, Mäder P. 2020. Enhanced soil quality with reduced tillage and solid
491 manures in organic farming – a synthesis of 15 years. *Sci Rep.* 10(1):4403. <https://doi.org/10.1038/s41598-020-61320-8>

492 Krueger ES, Ochsner TE. 2024. Traditional matric potential thresholds underestimate soil moisture at field capacity across
493 Oklahoma. *Soil Science Society of America Journal*. 88(5):1678–1690. <https://doi.org/10.1002/saj2.20733>

494 Lal R. 2009. Challenges and opportunities in soil organic matter research. *European Journal of Soil Science*. 60(2):158–169.
495 <https://doi.org/10.1111/j.1365-2389.2008.01114.x>

496 Lambert M-J, Traoré PCS, Blaes X, Baret P, Defourny P. 2018. Estimating smallholder crops production at village level from
497 Sentinel-2 time series in Mali's cotton belt. *Remote Sensing of Environment*. 216:647–657.
498 <https://doi.org/10.1016/j.rse.2018.06.036>

499 Lawal S, Sitch S, Lombardozzi D, Nabel JEMS, Wey H-W, Friedlingstein P, Tian H, Hewitson B. 2022. Investigating the
500 response of leaf area index to droughts in southern African vegetation using observations and model simulations. *Hydrology*
501 and *Earth System Sciences*. 26(8):2045–2071. <https://doi.org/10.5194/hess-26-2045-2022>

502 Lipiec J, Håkansson I, Tarkiewicz S, Kossowski J. 1991. Soil physical properties and growth of spring barley as related to the
503 degree of compactness of two soils. *Soil and Tillage Research*. 19(2):307–317. [https://doi.org/10.1016/0167-1987\(91\)90098-I](https://doi.org/10.1016/0167-1987(91)90098-I)

505 Mahmood S, Nunes MR, Kane DA, Lin Y. 2023. Soil health explains the yield-stabilizing effects of soil organic matter under
506 drought. *Soil & Environmental Health*. 1(4):100048. <https://doi.org/10.1016/j.seh.2023.100048>

507 Matiu M, Ankerst DP, Menzel A. 2017. Interactions between temperature and drought in global and regional crop yield
508 variability during 1961–2014. *PLOS ONE*. 12(5):e0178339. <https://doi.org/10.1371/journal.pone.0178339>

509 Meinke H, Hammer GL, van Keulen H, Rabbinge R, Keating BA. 1997. Improving wheat simulation capabilities in Australia
510 from a cropping systems perspective: water and nitrogen effects on spring wheat in a semi-arid environment. In: van Ittersum
511 MK, van de Geijn SC, editors. *Developments in Crop Science*. Vol. 25. Elsevier; p. 99–112. [https://doi.org/10.1016/S0378-519X\(97\)80012-8](https://doi.org/10.1016/S0378-519X(97)80012-8)

513 Minoli S, Jägermeyr J, Asseng S, Urfels A, Müller C. 2022. Global crop yields can be lifted by timely adaptation of growing
514 periods to climate change. *Nat Commun.* 13:7079. <https://doi.org/10.1038/s41467-022-34411-5>

515 Myneni RB, Ramakrishna R, Nemani R, Running SW. 1997. Estimation of global leaf area index and absorbed par using
516 radiative transfer models. *IEEE Transactions on Geoscience and Remote Sensing*. 35(6):1380–1393.
517 <https://doi.org/10.1109/36.649788>

518 Myneni RB, Williams DL. 1994. On the relationship between FAPAR and NDVI. *Remote Sensing of Environment*. 49(3):200–
519 211. [https://doi.org/10.1016/0034-4257\(94\)90016-7](https://doi.org/10.1016/0034-4257(94)90016-7)

520 Oldfield EE, Bradford MA, Wood SA. 2019. Global meta-analysis of the relationship between soil organic matter and crop
521 yields. *SOIL*. 5(1):15–32. <https://doi.org/10.5194/soil-5-15-2019>

522 Peng Y, Zhu T, Li Y, Dai C, Fang S, Gong Y, Wu X, Zhu R, Liu K. 2019. Remote prediction of yield based on LAI estimation
523 in oilseed rape under different planting methods and nitrogen fertilizer applications. *Agricultural and Forest Meteorology*.
524 271:116–125. <https://doi.org/10.1016/j.agrformet.2019.02.032>

525 Petcu E, Ion T, Pompiliu M, Petcu V. 2011. Effect of organic and conventional farming systems on some physiological
526 indicators of winter wheat. *Romanian Agricultural Research*. (28).

527 Porter JR, Gawith M. 1999. Temperatures and the growth and development of wheat: a review. *European Journal of Agronomy*.
528 10(1):23–36. [https://doi.org/10.1016/S1161-0301\(98\)00047-1](https://doi.org/10.1016/S1161-0301(98)00047-1)

529 Prabhakara K, Hively WD, McCarty GW. 2015. Evaluating the relationship between biomass, percent groundcover and remote
530 sensing indices across six winter cover crop fields in Maryland, United States. *International Journal of Applied Earth
531 Observation and Geoinformation*. 39:88–102. <https://doi.org/10.1016/j.jag.2015.03.002>

532 Punalekar SM, Verhoef A, Quaife TL, Humphries D, Bermingham L, Reynolds CK. 2018. Application of Sentinel-2A data
533 for pasture biomass monitoring using a physically based radiative transfer model. *Remote Sensing of Environment*. 218:207–
534 220. <https://doi.org/10.1016/j.rse.2018.09.028>

535 Pużyńska K, Synowiec A, Pużyński S, Bocianowski J, Klima K, Lepiarczyk A. 2021. The Performance of Oat-Vetch Mixtures
536 in Organic and Conventional Farming Systems. *Agriculture*. 11(4):332. <https://doi.org/10.3390/agriculture11040332>

537 R Core Team. 2022. R: The R Project for Statistical Computing [Internet]. [accessed 2023 Dec 22]. <https://www.r-project.org/>

538 Ray RL, Fares A, Risch E. 2018. Effects of Drought on Crop Production and Cropping Areas in Texas. *Agricultural &
539 Environmental Letters*. 3(1):170037. <https://doi.org/10.2134/ael2017.11.0037>

540 Revill A, Florence A, MacArthur A, Hoad SP, Rees RM, Williams M. 2019. The Value of Sentinel-2 Spectral Bands for the
541 Assessment of Winter Wheat Growth and Development. *Remote Sensing*. 11(17):2050. <https://doi.org/10.3390/rs11172050>

542 Rockström J. 2003. Resilience building and water demand management for drought mitigation. *Physics and Chemistry of the
543 Earth, Parts A/B/C*. 28(20):869–877. <https://doi.org/10.1016/j.pce.2003.08.009>

544 Rolli E, Marasco R, Vigani G, Ettoumi B, Mapelli F, Deangelis ML, Gandolfi C, Casati E, Previtali F, Gerbino R, et al. 2015.
545 Improved plant resistance to drought is promoted by the root-associated microbiome as a water stress-dependent trait.
546 *Environmental Microbiology*. 17(2):316–331. <https://doi.org/10.1111/1462-2920.12439>

547 Ru C, Hu X, Chen D, Wang W, Zhen J, Song T. 2023. Individual and combined effects of heat and drought and subsequent
548 recovery on winter wheat (*Triticum aestivum* L.) photosynthesis, nitrogen metabolism, cell osmoregulation, and yield
549 formation. *Plant Physiology and Biochemistry*. 196:222–235. <https://doi.org/10.1016/j.plaphy.2023.01.038>

550 Rubin RL, van Groenigen KJ, Hungate BA. 2017. Plant growth promoting rhizobacteria are more effective under drought: a
551 meta-analysis. *Plant Soil*. 416(1):309–323. <https://doi.org/10.1007/s11104-017-3199-8>

552 SCB. 1993. Jordbruksstatistisk årsbok 1993. Bulls Tryckeriaktiebolag.

553 SCB. 2018. Production of cereal crops, dried pulses and oilseed crops in 2018. *Statistiska meddelanden*. JO 19 SM 1801.

554 Seleiman MF, Al-Suhaibani N, Ali N, Akmal M, Alotaibi M, Refay Y, Dindaroglu T, Abdul-Wajid HH, Battaglia ML. 2021.
555 Drought Stress Impacts on Plants and Different Approaches to Alleviate Its Adverse Effects. *Plants*. 10(2).
556 <https://doi.org/10.3390/plants10020259>

557 Shankar T, Banerjee M, Malik GC, Dutta S, Maiti D, Maitra S, Alharby H, Bamagoos A, Hossain A, Ismail IA, EL Sabagh A.
558 2021. The Productivity and Nutrient Use Efficiency of Rice–Rice–Black Gram Cropping Sequence Are Influenced by Location
559 Specific Nutrient Management. *Sustainability*. 13(6):3222. <https://doi.org/10.3390/su13063222>

560 Sjulgård H, Colombi T, Keller T. 2022. Spatiotemporal patterns of crop diversity reveal potential for diversification in Swedish
561 agriculture. *Agriculture, Ecosystems & Environment*. 336:108046. <https://doi.org/10.1016/j.agee.2022.108046>

562 Sjulgård H, Keller T, Garland G, Colombi T. 2023. Relationships between weather and yield anomalies vary with crop type
563 and latitude in Sweden. *Agricultural Systems*. 211:103757. <https://doi.org/10.1016/j.agsy.2023.103757>

564 Sjulgård H. 2024. The potential of agricultural management to alleviate extreme weather impacts on Swedish crop production.
565 *Acta Universitatis Agriculturae Sueciae* (2024:84). <https://doi.org/10.54612/a.107ri2j3pt>

566 Skakun S, Vermote E, Franch B, Roger J-C, Kussul N, Ju J, Masek J. 2019. Winter Wheat Yield Assessment from Landsat 8
567 and Sentinel-2 Data: Incorporating Surface Reflectance, Through Phenological Fitting, into Regression Yield Models. *Remote
568 Sensing*. 11(15):1768. <https://doi.org/10.3390/rs11151768>

569 SMHI. 2018. Maj 2018 - Sommarvåder med rekordvärme | SMHI [Internet]. [accessed 2024 Oct 3].
570 [https://www.smhi.se/klimat/klimatet-da-och-nu/manadens-vader-och-vatten-sverige/manadens-vader-i-sverige/maj-2018-
571 sommarvader-med-rekordvarme-1.134781](https://www.smhi.se/klimat/klimatet-da-och-nu/manadens-vader-och-vatten-sverige/manadens-vader-i-sverige/maj-2018-sommarvader-med-rekordvarme-1.134781)

572 SMHI. 2023. Nedladdning av griddad nederbörd- och temperaturdata (PTHBV) [Internet]. [accessed 2023 Mar 8].
573 <https://www.smhi.se/data/ladda-ner-data/griddade-nederbord-och-temperaturdata-ptb>

574 Stockdale E a., Shepherd M a., Fortune S, Cuttle S p. 2002. Soil fertility in organic farming systems – fundamentally different?
575 *Soil Use and Management*. 18(s1):301–308. <https://doi.org/10.1111/j.1475-2743.2002.tb00272.x>

576 Stenberg M, Bjurling E, Gruvaeus I, Gustafsson K. 2005. Gödslingsrekommendationer och optimala kvävegivor för lönsamhet
577 och kväveeffektivitet i praktisk spannmålsodling. Skara: SLU.

578 Sun Q, Gilgen AK, Wittwer R, von Arx G, van der Heijden MGA, Klaus VH, Buchmann N. 2024. Drought effects on trait
579 space of winter wheat are independent of land management. *New Phytol*. 243(2):591–606. <https://doi.org/10.1111/nph.19851>

580 Verhoef W. 1998. Theory of radiative transfer models applied in optical remote sensing of vegetation canopies [PhD]. S.l.
581 Villegas D, Aparicio N, Blanco R, Royo C. 2001. Biomass Accumulation and Main Stem Elongation of Durum Wheat Grown
582 under Mediterranean Conditions. *Annals of Botany*. 88(4):617–627. <https://doi.org/10.1006/anbo.2001.1512>

583 de Vries FT, Griffiths RI, Knight CG, Nicolitch O, Williams A. 2020. Harnessing rhizosphere microbiomes for drought-
584 resilient crop production. *Science*. 368(6488):270–274. <https://doi.org/10.1126/science.aaz5192>

585 Waldner F, Horan H, Chen Y, Hochman Z. 2019. High temporal resolution of leaf area data improves empirical estimation of
586 grain yield. *Sci Rep*. 9(1):15714. <https://doi.org/10.1038/s41598-019-51715-7>

587 Wang B, Liu DL, Asseng S, Macadam I, Yu Q. 2017. Modelling wheat yield change under CO₂ increase, heat and water stress
588 in relation to plant available water capacity in eastern Australia. European Journal of Agronomy. 90:152–161.
589 <https://doi.org/10.1016/j.eja.2017.08.005>

590 Wang E, Cresswell H, Xu J, Jiang Q. 2009. Capacity of soils to buffer impact of climate variability and value of seasonal
591 forecasts. Agricultural and Forest Meteorology. 149(1):38–50. <https://doi.org/10.1016/j.agrformet.2008.07.001>

592 Wasaya A, Rehman I, Mohi Ud Din A, Hayder Bin Khalid M, Ahmad Yasir T, Mansoor Javaid M, El-Hefnawy M, Brestic M,
593 Rahman MA, El Sabagh A. 2023. Foliar application of putrescine alleviates terminal drought stress by modulating water status,
594 membrane stability, and yield- related traits in wheat (*Triticum aestivum* L.). Frontiers in Plant Science. 13.

595 Watson DJ. 1947. Comparative Physiological Studies on the Growth of Field Crops: I. Variation in Net Assimilation Rate and
596 Leaf Area between Species and Varieties, and within and between Years. Annals of Botany. 11(1):41–76.
597 <https://doi.org/10.1093/oxfordjournals.aob.a083148>

598 Wocher M, Berger K, Danner M, Mauser W, Hank T. 2020. RTM-based dynamic absorption integrals for the retrieval of
599 biochemical vegetation traits. International Journal of Applied Earth Observation and Geoinformation. 93:102219.
600 <https://doi.org/10.1016/j.jag.2020.102219>

601 Yamamoto S, Hashimoto N, Homma K. 2023. Evaluation of LAI Dynamics by Using Plant Canopy Analyzer and Its
602 Relationship to Yield Variation of Soybean in Farmer Field. Agriculture. 13(3):609.
603 <https://doi.org/10.3390/agriculture13030609>

604 Zhang J, Zhang S, Cheng M, Jiang H, Zhang X, Peng C, Lu X, Zhang M, Jin J. 2018. Effect of Drought on Agronomic Traits
605 of Rice and Wheat: A Meta-Analysis. International Journal of Environmental Research and Public Health. 15(5):839.
606 <https://doi.org/10.3390/ijerph15050839>

607 Zipper SC, Qiu J, Kucharik CJ. 2016. Drought effects on US maize and soybean production: spatiotemporal patterns and
608 historical changes. Environ Res Lett. 11(9):094021. <https://doi.org/10.1088/1748-9326/11/9/094021>

609 Zuber V, Strimmer K. 2011. High-Dimensional Regression and Variable Selection Using CAR Scores. Statistical Applications
610 in Genetics and Molecular Biology. 10(1). <https://doi.org/10.2202/1544-6115.1730>